An Update to E12-11-007
Asymmetries in Semi-Inclusive Deep-Inelastic $(e, e'\pi^{\pm})$ Reactions on a Longitudinally Polarized ^{3}He Target at 8.8 and 11 GeV

J.-P. Chen, J. Huang (Contact),* Y. Qiang, and W. B. Yan
Co-spokespersons

the E12-11-007 collaboration
(The full author list can be found in the original proposal)

and the Hall A collaboration

ABSTRACT

This is an update for E12-11-007[1], which was approved by PAC 37 in Jan 2011. E12-11-007 will measure single-target and double spin azimuthal asymmetries (SSAs and DSAs) in semi-inclusive electroproduction of charged pions using the upgraded CEBAF electron beam, a longitudinally polarized ^{3}He target as an effective polarized neutron target, and the recently approved SoLID (Solenoidal Large Intensity Device) spectrometer [1]. We also request a high beam polarization for both this experiment and E12-10-006. The SSAs and DSAs, with longitudinal and transverse target spin, respectively, are related to two T-even "worm-gear" transverse-momentum-dependent parton distributions (TMD) of the nucleon at leading twist. Both of the "worm-gear" TMD, g_{1T} (or transversal helicity) and $h_{1L}^{\perp}$ (or longitudinal transversity), require an interference between wave function components that differ by one unit of quark orbital angular momentum (OAM) as explicitly shown in several models. The experimental information on the "worm-gear" TMDs will be used to test Lattice QCD calculations, quark-gluon correlations and generic model assumptions of the nucleon system. In addition, the DSAs with a longitudinal target spin will constrain the flavor decomposition of the quark helicity distribution of the nucleon and provide information on their transverse momentum dependence. This experiment will provide the first data on SIDIS target-SSA with a longitudinally polarized effective neutron target. All asymmetries will be measured with a high precision and a large kinematic coverage in a 4-D phase space of x, z, $P_{h\perp}$ and Q^2. The systematic uncertainties are minimized by using fast target spin flips and a large coverage in the azimuthal angles. We request 35 PAC days of beam on a longitudinally polarized ^{3}He target.

* jinhuang@jlab.org
[1] The original proposal can be found at
http://www.jlab.org/exp_prog/PACpage/PAC37/proposals/Proposals/New%20Proposals/PR-11-007.pdf

I. SCIENTIFIC CASE

I.1. "Worm-Gears" Distributions

I.1.1. "Worm-gear" Functions and Their Relation to Quark Orbital Motion

In recent years, a new phase of investigation of nucleon structure has been started by studying physical observables that are sensitive to the transverse momentum structure of nucleons. This information is encoded in the Transverse Momentum Dependent parton distributions (TMDs), which describe the spin-correlated three-dimensional momentum structure of the nucleon's quark and gluon constituents [2, 3]. At leading twist, there are eight quark TMDs. They are functions of x, Q^2 and the quark transverse momentum, $\boldsymbol{p}_T$. Three of them (the unpolarized distribution, f_1; the helicity, g_{1L}; and the transversity distributions, h_1) survive the integration over $\boldsymbol{p}_T$, while the other five vanish. These five TMDs provide novel information on the spin-orbit correlations. Of the five distributions, the T-even "Worm-gear" functions, g_{1T} (or transversal helicity) and $h_{1L}^{\perp}$ (or longitudinal transversity), describe the probability of finding a longitudinally polarized quark inside a transversely polarized nucleon and a transversely polarized quark inside a longitudinally polarized nucleon, respectively. They give the strength of dipole contributions and correspond to matrix elements involving one unit of helicity flip, either on the nucleon side (g_{1T}) or on the quark side ($h_{1L}^{\perp}$) [4].

Both g_{1T} and $h_{1L}^{\perp}$ provide unique information on the quark spin-orbital correlations. They represent the real part of an interference between nucleon wave functions that differ by one unit of orbital angular momentum, while the imaginary parts are related to the better studied $f_{1T}^{\perp}$ (Sivers functions) and $h_1^{\perp}$ (Boer-Mulders functions) [5, 6]. Model studies show that g_{1T} and $h_{1L}^{\perp}$ come mainly from the interference between $L = 0$ and $L = 1$ states [7–9] and a small contribution from an interference between $L = 1$ and $L = 2$ states [8].

The spin-dependent distributions in transverse-momentum space have an analogy in terms of spin-dependent distributions in impact parameter space, which are described by generalized parton distributions. This correspondence hold for 6 of the leading-twist TMDs, but not for the two "worm-gear" TMDs because of time-reversal symmetry [10–12]. Therefore, the "worm-gear" functions can not be generated dynamically from coordinate space densities by final-state interactions. Their appearance may be seen as a genuine sign of intrinsic transverse motion of the quarks [13].

Semi-inclusive DIS (SIDIS), in which a hadron from the fragmentation of the struck quark is detected in coincidence with the scattered lepton, provides access to all leading twist TMDs [14]. Especially for this experiment, $h_{1L}^{\perp}$ will be accessed in the SIDIS target single spin asymmetry, $A_{UL}^{\sin 2\phi_h}$ with a longitudinally polarized target, which is proportional to the convolution between $h_{1L}^{\perp}$ and Collins fragmentation function, $H_1^{\perp}$. The helicity and g_{1T} distribution can be accessed through beam-target double spin asymmetries, A_{LL} and $A_{LT}^{\cos(\phi_h-\phi_S)}$,

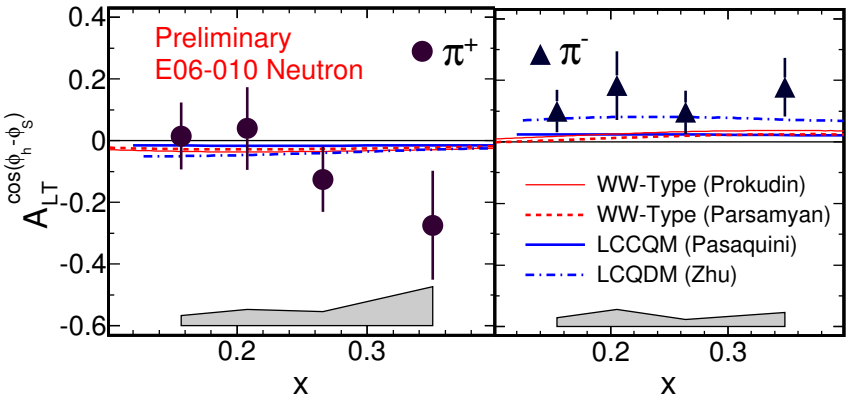

Figure 1. Preliminary results of the first neutron A_{LT} measurement by E06-010 [17], which were compared to model calculations of to several model calculations, including a light-cone constituent quark model (LCCQM) [7, 8], a light-cone quark-diquark model (LCQDM) [18] and WW-type approximations with parametrizations from Ref. [15] and Ref. [16].

with a longitudinally and transversely polarized targets, respectively. The "worm-gear" and helicity TMDs are T-even. Therefore, the effects from the T-odd FSIs are expected to be suppressed.

Recently, the E06-010 collaboration released the preliminary results on the first neutron A_{LT} measurement (Fig. 1). The data are consistent in sign with the model predictions [7, 8, 15, 16], but favor a larger magnitude for the π^- production, and therefore suggest at leading twist a larger g_{1T} than the contemporary model calculations. This experiment has demonstrated the power of polarized ^{3}He as an effective polarized neutron target, and has laid the foundation for future high-precision measurements of neutron TMDs using a polarized ^{3}He target and SoLID following the JLab 12 GeV upgrade.

I.1.2. Lattice Calculation

Recently, TMD was explored for the first time using lattice QCD [13, 19], making use of a simplified definition of TMDs with straight gauge links. The "worm-gear" functions were the first spin-polarized TMDs addressed with this method. They give rise to a dipole deformation of the density of quarks in the transverse momentum plane. The size of the dipole deformation can be characterized by an average transverse momentum shift, which is related to a valance-quark-like moment of the worm-gear distributions. The results [13, 19] show that u-quarks have a larger shift than d-quarks with opposite signs and $g_{1T} \approx -h_{1L}^{\perp}$, both of which were supported by a large spectrum of models as discussed in Sec. I.1.4. Model-assisted extractions of the momentum shift can be accomplished with this proposed measurement by

taking advantage of the high precision and large kinematic coverage.

I.1.3. Relation to Collinear PDFs

Using the Lorentz Invariance Relations (LIRs) [2] and the Wandzura and Wilczek (WW) approximation [20–22], the "worm-gear" functions can be related to the better understood collinear parton distribution functions (PDF), g_1 and h_1:

$$g_{1T}^{q(1)}(x) \overset{WW-type}{\approx} x\int_x^1 \frac{dy}{y} g_1^q(y) \tag{1}$$

$$h_{1L}^{\perp q(1)}(x) \overset{WW-type}{\approx} -x^2\int_x^1 \frac{dy}{y^2} h_1^q(y). \tag{2}$$

A precise extraction of g_{1T} and $h_{1L}^{\perp}$ and comparison to these calculation are highly desirable, which can verify the following approximations and relations experimentally:

- WW approximation and LIRs are based on assumptions that the twist-3 "interaction dependent" terms due to quark-gluon correlations and current quark mass terms are small [21, 22].
- The measurement on $h_{1L}^{\perp}$ will provide a constrain on the Transversity distribution h_1.

I.1.4. Test of Models and Relations among TMDs

The "worm-gear" distributions were predicted by a number of models, of which several predictions were made for this experiment as shown in Fig. 12 and 13 of the original proposal. Common features of these estimations suggest that g_{1T}^u is positive, g_{1T}^d is negative, and the peak amplitude of g_{1T}^u is predicted to be larger than g_{1T}^d. g_{1T} and $h_{1L}^{\perp}$ reach their maximum values in the valence quark region at a level of a few percent relative to the unpolarized distribution f_1^q.

Recently, C. Lorcé and B. Pasquini reviewed the model relations among TMDs and their origins, which were predicted by a large class of models [23]. These model relations have essentially a geometrical origin and can be traced back to properties of rotational invariance of the system. Generally, however, the relations do not hold exactly in QCD. Experimental information on these TMDs can test the generic model assumptions, which are shared by the supporting models.

The most simple one of the model relations,

$$g_{1T}^q = -h_{1L}^{\perp q} \tag{3}$$

which is flavor-independent, can be tested by this experiment within identical kinematic regions. Pioneering calculations in lattice QCD give indications that the relation (3) may indeed be approximately satisfied [13, 19]. The experimental test that to which extent Eq. (3) is conserved or broken can help to study the validity of rest of the flavor-independent relations, $h_1^q + \frac{\boldsymbol{k}_\perp^2}{2M^2}\, h_{1T}^{\perp q} = g_{1L}^q$ and $(g_{1T}^q)^2 + 2h_1^q\, h_{1T}^{\perp q} = 0$. These relations can be further used to make predictions in a generic way for the Pretzelosity distribution, $h_{1T}^{\perp q}$, which is experimentally challenging to measure due to the small values of the predicted asymmetries.

I.2. Helicity Distributions

In parallel to the A_{UL} measurement, this experiment will provide high precision data on the neutron A_{LL} asymmetry. Once included in the global analysis, these results will significantly improve the precision of the polarized PDF for Δd. In addition, existing data [24] and models [16, 25] suggested a $P_{h\perp}$ dependence on A_{LL}. A possible interpretation of the $P_{h\perp}$-dependence of the double-spin asymmetry may involve different widths of the transverse momentum distributions of quarks with different flavor and polarizations [25] resulting from different orbital motion of quarks polarized in the direction of the nucleon spin [26]. Clear correlations between quark helicity and transverse momentum are present in model calculations [9, 27] and lattice QCD studies [19]. This experiment will provide conclusive $P_{h\perp}$-dependency with high statistics and a broad x, Q^2 and z coverage.

I.3. Proposed Measurement

The experimental setup will be largely shared with experiment E12-10-006 [28] with an addition of a longitudinally polarized target. The polarized ^{3}He target will be used as an effective polarized neutron target. Its specification, which was achieved in the recently completed neutron Transversity experiment [29], includes the capability of polarizing in both longitudinal and transverse spin directions, a luminosity of $10^{36}\,(n)\,/\mathrm{cm}^2/s$, 60% target polarization and fast target spin reversals. The SoLID spectrometer, which consists of a superconducting solenoid magnet, a detector system of forward-angle detectors and large-angle detectors, will be shared by both approved SoLID SIDIS experiments [28, 30] and in large part shared by the PVDIS experiment [31]. The kinematic coverage will cover the valance quark region, $x = 0.05$-0.65 at $Q^2 = 1.0$-$8.0\,(\mathrm{GeV})^2$. A large range of hadron transverse momentum, $P_{h\perp} = 0$-$1.6\,\mathrm{GeV}$, will be covered. We choose the leading pions with $0.3 < z < 0.7$ to favor the current fragmentation, while data beyond this z cuts will provide information on backgrounds of the resonance region and of the target fragmentation region.

We request 35 PAC days of polarized beam on the longitudinal polarized target. As shown in Fig. 12 to 14 (for a single $z - Q^2$ bin) and Fig. 15 to 20 (all bins) of the original proposal,

the data for the SIDIS $\pi^{\pm}$ productions are binned in more than 1000 bins covering a 4-D phase space of x, z, $P_{h\perp}$ and Q^2 with a typical statistical precision of 0.5% (absolute, on the neutron). The systematical uncertainty is 7% (relative) as shown in Table III of the original proposal.

I.4. Complementary Data in Proton (Issue Raised in the PAC 37 Report)

For each of the asymmetries measured in this experiment, data for π^+ and π^- production will be taken simultaneously with an equivalent kinematic coverage and precision, which will provide two constrains in decomposing the asymmetries into contributions from different quark flavors. Furthermore, to achieve a comprehensive view of the targeted TMDs in the quark flavor decomposition, data from longitudinally and transversely polarized proton targets will be needed. The longitudinally polarized proton data with a 6GeV beam were provided by the CLAS collaboration [24]. The precision on that measurement will be significantly improved by CLAS12 E12-07-107 [32], which will cover in a similar kinematic region as this experiment. A joint global analysis between this experiment and E12-07-107 will provide a good understanding on $h_{1L}^{\perp q}$ with some model assistance. A future high precision and multi-dimensional mapping of proton A_{UL} will fully complement this measurement and minimize the assumptions in the global analysis and provide an ultimate understanding of $h_{1L}^{\perp q}$ in this kinematic region. In addition, a proposal is being prepared for PAC 38 using a transversely polarized proton target with the SoLID setup, which can provide the matching complementary data regarding g_{1T}.

II. TECHNICAL PROGRESS

II.1. Magnet Choice

Studies were performed comparing the merits of the possible magnet options for SoLID. Simulation tools were setup and magnetic field maps were generated with a 2-D program Poisson [33]. GEANT simulations were developed with the BaBar, CLEO, CDF and the ZEUS magnets [34, 35]. The Hall D magnets (both the refurbished one and the new design) were considered. It was concluded that the BaBar and CLEO magnets are the best options which satisfy both PVDIS and SIDIS experiments without compromising the physics goal and have the flexibility for future expansion of the physics program. $P_{h\perp}$ and Q^2 coverage may be reduced for CDF and ZEUS magnet, while the majority of the kinematic range remains same. Active efforts have been made in pursuing the magnets with strong support from the Jefferson Lab management.

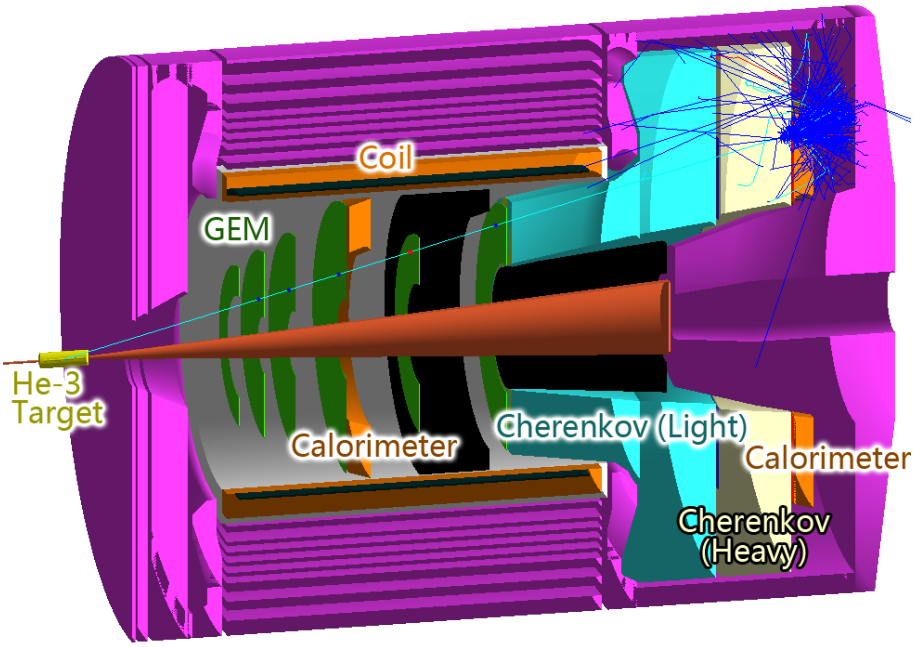

Figure 2. A typical event display for SoLID in GEMC. See text for description of the detectors.

II.2. Geant4 Based Simulation

The collaboration has made significant progress on the SoLID simulation. The framework has been switched from a Geant3 based program COMGEANT to a Geant4 based GEMC [36] package, which has been successfully used for CLAS12 simulations in the JLab Hall B 12GeV upgrade. The program provides both interactive mode for visualizing in 3D and batch mode for mass running. In the SoLID GEMC simulation framework, both detector components and detector response can be turned on/off or customized during run time. This flexibility enables us to have individual detector simulation and the whole SoLID simulation in one unified framework. A typical event display is shown in Fig. 2. The solenoid magnet coil, yoke and detector configurations have been produced for the magnet options of BaBar, CLEO, CDF and ZEUS. The SIDIS kinematic distribution have been studied for various magnets and have helped us identify the favorable magnet choice. The low energy background is also studied, which provided crucial guidance to the design of all the detector systems.

II.3. Calorimeter

As shown in Fig. 2, two sets of electromagnetic calorimeters will be used to identify electron signals in the forward and large-angle sides by measuring the energy deposition in the calorimeter through the electromagnetic shower. For the electron sample, a pion rejection of

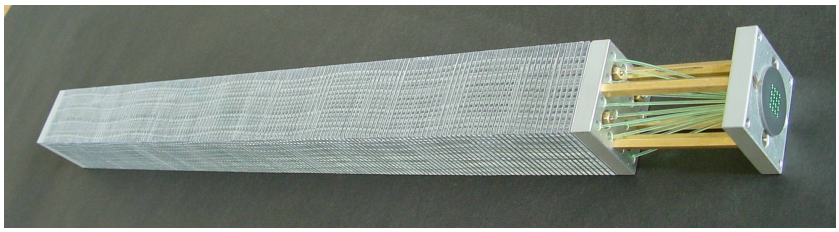

Figure 3. A Shashlyk calorimeter module produced by IHEP for the COMPASS experiment.

100:1 will be provided by the calorimeters with a pre-shower/shower splitting. Two options of calorimeter will satisfy the need of the SoLID experiments: Shashlyk type calorimeter [37] and the lead/scintillating fiber calorimeter [38]. The Shashlyk type calorimeter is favored for SoLID due to the reasons of its compact light read out and the maturity in mass production.

The Shashlyk type calorimeter is a sampling calorimeter constructed from alternating layers of scintillator and heavy absorber. Scintillation light is absorbed, re-emitted and transported to the photon detector by wave-length shifting optical fibers penetrating through the calorimeter modules longitudinally (along the beam direction). The plastic scintillator group in the Institute for High Energy Physics (IHEP) of Russia has extensive experience of R&D and mass production of Shashlyk type calorimeters. The group has successfully developed the Shashlyk calorimeter for the KOPIO experiment [37, 39] and worked on building the PANDA [40] and COMPASS calorimeters (Fig. 3). Multiple degrees of flexibility in customizing the modules are offered by IHEP. A Geant4 simulation was used to study the optimal key specifications, to balance between higher pion rejection and lower cost:

Absorber thickness per layer: each layer consists of a 1.5 mm-thick scintillator plate and an absorber plate made of lead. To reach the required pion rejection, the Pb absorber thickness of 0.6 mm or less is favored to provide a fine sampling, and therefore an energy resolution of $\lesssim 5\%/\sqrt{E}$. For a 0.6 mm-Pb configuration, the effective radiation length (X_0) is about 21 mm.

Longitudinal size: a total thickness of about 20 X_0 and a pre-shower thickness of $3 \sim 5\,X_0$ can maximize the difference in energy deposition between electrons and pions at the momentum ranges for SoLID.

Lateral size: the lateral size of each module determines the position resolution and the background level of the reconstructed shower hits. It is also the most relevant factor to the overall cost of the calorimeter. The study showed that a lateral size of about 10 cm will provide a good balance between position resolution and cost.

We will collaborate with IHEP closely and further study the design for both calorimeters. Prototypes will be tested at JLab and mass production will be held at IHEP.

II.4. DAQ System

The DAQ system of SoLID will utilize the recently developed high speed, fully pipelined VME Switched Serial (VXS) modules by Jefferson Lab DAQ group. The payload modules include FADC250, a 16-channel 12-bit ADC sampling at 250 MHz and F1-TDC, a 32 channel TDC with 60 ps resolution. The trigger will be generated and distributed by the following modules: Crate Trigger Processor (CTP), Sub-System Processor (SSP), Global Trigger Processor (GTP), Trigger Supervisor (TS), Trigger Interface/Distribution (TID) and Signal Distribution (SD) modules.

Taking the advantages of the programmable onboard FPGA chips on the modules at various stages, the raw signals can be conditioned in real time (every 4 ns) and a hit pattern (can be used for pattern match or coincidence) or a sum or their combination will first be generated from individual sub-system, then such information will be gathered and a global hit pattern or sum or certain combination will be calculated for the final L1 trigger pattern. The fast communications inside each VXS crate and between crates ($\sim$10 Gbps) ensure enough bandwidth to realize such a task.

The main L1 trigger of the SoLID SIDIS experiments will be the coincidence of an electron hit in either the forward or the large angle region and a charged particle hit in the forward detector. The estimated rate will be about 50 kHz with a 36 ns coincidence window. Considering the multiplicity in the individual detectors, the average size of each event is about 4 kB, and the total raw data rate is expected to be 200 MB/s. Such a data rate will not challenge the transfer speed of the VXS system. But in order to reduce the disk space needed to save the raw data, an L3 farm, similar to what Hall D will use during its high luminosity running, using parallel computing technique can be built to further reject the accidental events. A rejection ratio is expected to be greater than 5:1.

II.5. Other Technical Updates

More detailed discussions for this section can be found in the PAC 38 update to E12-10-006.

Tracking Detector: The SoLID spectrometer requires high resolution track reconstruction under high rate conditions over a large area. A cost effective solution for large-area tracking in a high-rate environment is provided by the Gas Electron Multiplier (GEM). Four of the groups responsible for GEM chambers of SoLID, CIAE (Li group)), INFN (Cisbani group), UVa (Liyanage group), and USTC (Zhao group) are members of the RD-51 collaboration, which developed and shared the GEM technology. Prototypes have been constructed by UVa and INFN. We are planning a test run with the 10 cm$\times$10 cm tracker plus the two 40$\times$50 cm^2 GEM chambers in Hall A during the g2p/GEp experiment scheduled for the winter of 2011.

Cerenkov Detector: Two Cerenkov detectors will provide PID information: a light-gas Cherenkov for electron ID and a heavy-gas Cherenkov for pion ID. Recently a Geant4 simulation was used to optimize the design of the optical system. For the light-gas Cherenkov, it was found that with just one system of 30 spherical mirrors (following the SoLID sectoring) near perfect collection efficiency, >95%, can be achieved with a 12" by 12" photon detector (active area). Two options have been considered for the photon detectors: magnetic field resistant photomultiplier tubes, to be used in combination with Winston cones, and GEM with Cesium Iodide coating.

MRPC: A prototype is currently being built at TSU for a beam test in Hall A during the fall of 2011.

III. SUMMARY

We propose a measurement of the neutron azimuthal asymmetries of $A_{UL}^{\sin 2\phi_h}$ and A_{LL} in semi-inclusive electroproduction of charged pions for 35 PAC days using the polarized CEBAF electron beam, the Hall A polarized ^{3}He target and the approved SoLID spectrometer. In addition, high beam polarization for experiment E12-10-006 is requested to measure the beam-target double spin asymmetry, $A_{LT}^{\cos(\phi_h-\phi_S)}$. All the asymmetries will be measured in four dimensional binning with ultimate high precision. The kinematics will focus on the valence quark region. The $A_{UL}^{\sin 2\phi_h}$ and $A_{LT}^{\cos(\phi_h-\phi_S)}$ asymmetries are related to two "worm-gear" TMD of nucleons, $h_{1L}^{\perp}$ and g_{1T}. With the immense coverage and the extraordinary precision, the data from this experiment will provide important and unique information to understand the correlations between the quark orbital angular momentum, the nucleon spin and the quark spin. In addition, A_{LL} data will significantly improve the precision of the global analysis on the helicity distributions and their transverse momentum dependence, especially for the d quark.

This measurement will share the setup with experiment E12-10-06 [28] besides an additional requirement of a longitudinally polarized target. Steady progress has been made in the detector designs. Together, the SoLID SIDIS experiments will define the precision of world data of SIDIS on an effective polarized neutron target.

[1] H. Gao *et al.*, Eur. Phys. J.Plus **126**, 1 (2011), arXiv:1009.3803 [hep-ph].
[2] P. J. Mulders *et al.*, Nucl. Phys. **B461**, 197 (1996), arXiv:hep-ph/9510301.
[3] D. Boer and P. J. Mulders, Phys. Rev. **D57**, 5780 (1998), arXiv:hep-ph/9711485.
[4] C. Lorce *et al.*, JHEP **05**, 041 (2011), arXiv:1102.4704 [hep-ph].
[5] A. Bacchetta *et al.*, Phys. Rev. Lett. **85**, 712 (2000), arXiv:hep-ph/9912490 [hep-ph].

[6] X.-d. Ji *et al.*, Nucl. Phys. **B652**, 383 (2003), arXiv:hep-ph/0210430 [hep-ph].

[7] B. Pasquini and othersb, Phys. Rev. **D78**, 034025 (2008), arXiv:0806.2298 [hep-ph].

[8] S. Boffi *et al.*, Phys. Rev. **D79**, 094012 (2009), arXiv:0903.1271 [hep-ph].

[9] A. Bacchetta *et al.*, Eur. Phys. J. **A45**, 373 (2010), arXiv:1003.1328 [hep-ph].

[10] M. Diehl and P. Hagler, Eur. Phys. J. **C44**, 87 (2005), arXiv:hep-ph/0504175 [hep-ph].

[11] B. Pasquini and C. Lorce, (2010), arXiv:1008.0945 [hep-ph].

[12] B. Pasquini and C. Lorce, in *GPD workshop at Trento*, edited by a (2010).

[13] P. Hagler *et al.*, Europhys. Lett. **88**, 61001 (2009), arXiv:0908.1283 [hep-lat].

[14] A. Bacchetta *et al.*, JHEP **02**, 093 (2007), arXiv:hep-ph/0611265.

[15] A. Kotzinian *et al.*, Phys. Rev. **D73**, 114017 (2006), arXiv:hep-ph/0603194 [hep-ph].

[16] H. Avakian, A. Kotzinian, B. U. Musch, A. Prokudin, and P. Schweitzer, (2011), in Preparation.

[17] J. Huang, in *XIX International Workshop on Deep-Inelastic Scattering and Related Subjects (DIS 2011)* (2011).

[18] J. Zhu and B.-Q. Ma, Phys. Lett. **B696**, 246 (2011).

[19] B. U. Musch *et al.*, Phys. Rev. **D83**, 094507 (2011), arXiv:1011.1213 [hep-lat].

[20] S. Wandzura and F. Wilczek, Phys. Lett. **B72**, 195 (1977).

[21] H. Avakian *et al.*, Phys. Rev. **D77**, 014023 (2008), arXiv:0709.3253 [hep-ph].

[22] A. Metz *et al.*, Phys. Lett. **B680**, 141 (2009), arXiv:0810.5212 [hep-ph].

[23] C. Lorce and B. Pasquini, (2011), arXiv:1104.5651 [hep-ph].

[24] H. Avakian *et al.* (CLAS), Phys. Rev. Lett. **105**, 262002 (2010), arXiv:1003.4549 [hep-ex].

[25] M. Anselmino *et al.*, Phys. Rev. **D74**, 074015 (2006), arXiv:hep-ph/0608048 [hep-ph].

[26] H. Avakian *et al.*, Phys. Rev. Lett. **99**, 082001 (2007), arXiv:0705.1553 [hep-ph].

[27] H. Avakian *et al.*, Phys. Rev. **D81**, 074035 (2010), arXiv:1001.5467 [hep-ph].

[28] J. P. Chen, H. Gao, X. Jiang, J. Peng, X. Qian, and et al, "JLab E12-10-006 : Target Single Spin Asymmetry in Semi-Inclusive Deep-Inelastic Electro Pion Production on a Trasversely Polarized 3He Target at 8.8 and 11 GeV, An update to PR12-09-014," (2010).

[29] X. Qian *et al.*, (2011), arXiv:1106.0363 [nucl-ex].

[30] J. P. Chen, H. Gao, X. Jiang, J. Peng, X. Qian, and et al, "JLab PR12-09-014 : Target Single Spin Asymmetry in Semi-Inclusive Deep-Inelastic Electro Pion Production on a Trasversely Polarized 3He Target at 11 GeV," (2010).

[31] P. Souder *et al.*, "JLab E12-10-007 : Precision Measurement of Parity-Violation in Deep Inelastic Scattering Over a Broad Kinematic Range," (2010).

[32] H. Avakian, P. Bosted, K. Griffioen, K. Hafidi, P. Rossi, and et al, "JLab E12-07-107 : Studies of Spin-Orbit Correlations with Longitudinally Polarized Target," (2007).

[33] P. Reimer, Z. Zhao, *et al.*, "Possion simulation of possible magnet for solid," Hall A Wiki.

[34] Z. Zhao, in *Solid Collaboration Meeting, June 2011* (2011).

[35] H. Gao, in *Solid Collaboration Meeting, June 2011* (2011).

[36] M. Ungaro *et al.*, "GEMC (GEant4 Monte-Carlo) framework," Website, https://gemc.jlab.org/.

[37] G. Atoian *et al.*, Nucl. Instrum. Meth. **A584**, 291 (2008), arXiv:0709.4514 [physics.ins-det].

[38] D. Hertzog *et al.*, Nucl. Instrum. Meth. **A294**, 446 (1990).

[39] Y. Kharlov *et al.*, Nucl. Instrum. Meth. **A606**, 432 (2009), arXiv:0809.3671 [physics.ins-det].

[40] D. Morozov *et al.*, J. Phys. Conf. Ser. **160**, 012021 (2009).